

Acetonitrile-Vapor-Induced Color and Luminescence Changes in a Cyclometalated Heteroleptic Iridium Complex

Zhiwei Liu, Zuqiang Bian,* Jiang Bian, Zhendong Li, Daobo Nie, and Chunhui Huang*

Beijing National Laboratory for Molecular Sciences (BNLMS), State Key Laboratory of Rare Earth Materials Chemistry and Applications, College of Chemistry and Molecular Engineering, Peking University, Beijing, People's Republic of China 100871

Received October 30, 2007

An iridium complex $\text{PIr}(\text{qnx})$ (iridium(III) bis(2-phenylpyridinato- N,C^2)(quinoxaline-2-carboxylate)) is reported for its unique and fast vapochromic and vapoluminescent behaviors. The emission of $\text{PIr}(\text{qnx})$ is governed by the whole crystal rather than the individual molecule. $\text{PIr}(\text{qnx})$ has been found to exist as both black and red forms in the solid state. The black form can be transformed into the red form upon its exposure to acetonitrile or propionitrile vapor, whereas no response was observed when it was exposed to other volatile organic compounds. To understand the vapochromic and vapoluminescent behaviors, we determined crystal structures of both forms by X-ray diffraction. In addition, we employed density functional theory in investigating weak intermolecular interactions, such as hydrogen bonding and $\pi-\pi$ interactions in the two forms.

Introduction

Vapochromic and vapoluminescent materials, namely, those capable of detecting volatile organic compounds (VOCs) via changes in color and luminescence with fast response times, are attracting increasing attention because of their potential practical sensor applications. Until now, many transition-metal complexes, such as zinc,^{1,2} gold,^{3,4} palladium, and platinum,^{5–14} have been investigated as vapochromic and vapoluminescent materials. The VOC-

induced responses usually originate from a change in the metal–metal distances and $\pi-\pi$ interactions in the excited state of the complexes, and most of them simultaneously respond to many VOCs by demonstrating vapochromic behavior, vapoluminescent behavior, or both.^{3,4,10,11}

Recently, many cyclometalated heteroleptic iridium complexes $\text{Ir}(\text{C}^{\wedge}\text{N})_2(\text{LX})$ (where $\text{C}^{\wedge}\text{N}$ stands for cyclometalated ligand, such as 2-phenylpyridine, and LX stands for ancillary ligand, such as acetyl acetonate) have been investigated in order to exploit the high photoluminescence (PL) efficiency of this type of complex.^{15–19} Acetyl acetonate (acac) was most often chosen as LX because of its high triplet energy level; thus the efficient phosphorescence comes from ligand centered $^3(\pi-\pi^*)$ and $^3\text{MLCT}$ (triplet metal-to-ligand charge transfer) excited states.¹⁵ However, if the triplet energy level of the ancillary ligand was adjusted or if hydrogen bonding

* To whom correspondence should be addressed. E-mail: chuang@pku.edu.cn (C.H.). Tel: +86-10-62757156. Fax: +86-10-62757156.

- (1) Pang, J.; Marcotte, E. J.-P.; Seward, C.; Brown, R. S.; Wang, S. *Angew. Chem., Int. Ed.* **2001**, *40*, 4042.
- (2) Das, S.; Bharadwaj, P. K. *Inorg. Chem.* **2006**, *45*, 5257.
- (3) Vickery, J. C.; Olmstead, M. M.; Fung, E. Y.; Balch, A. L. *Angew. Chem., Int. Ed. Engl.* **1997**, *36*, 1179.
- (4) Mansour, M. A.; Connick, W. B.; Lachicotte, R. J.; Gysling, H. J.; Eisenberg, R. *J. Am. Chem. Soc.* **1998**, *120*, 1329.
- (5) Albrecht, M.; Lutz, M.; Spek, A. L.; van Koten, G. *Nature* **2000**, *406*, 970.
- (6) Kunugi, Y.; Mann, K. R.; Miller, L. L.; Exstrom, C. L. *J. Am. Chem. Soc.* **1998**, *120*, 589.
- (7) Buss, C. E.; Anderson, C. E.; Pomije, M. K.; Lutz, C. M.; Britton, D.; Mann, K. R. *J. Am. Chem. Soc.* **1998**, *120*, 7783.
- (8) Buss, C. E.; Mann, K. R. *J. Am. Chem. Soc.* **2002**, *124*, 1031.
- (9) Grove, L. J.; Rennekamp, J. M.; Jude, H.; Connick, W. B. *J. Am. Chem. Soc.* **2004**, *126*, 1594.
- (10) Wadas, T. J.; Wang, Q.-M.; Kim, Y.-j.; Flaschenreim, C.; Blanton, T. N.; Eisenberg, R. *J. Am. Chem. Soc.* **2004**, *126*, 16841.
- (11) Kato, M.; Omura, A.; Toshikawa, A.; Kishi, S.; Sugimoto, Y. *Angew. Chem., Int. Ed.* **2002**, *41*, 3183.
- (12) Che, C.-M.; Fu, W.-F.; Lai, S.-W.; Hou, Y.-J.; Liu, Y.-L. *Chem. Commun.* **2003**, 118.

- (13) Lu, W.; Chan, M. C. W.; Zhu, N.; Che, C. M.; He, Z.; Wong, K. Y. *Chem.–Eur. J.* **2003**, *9*, 6155.
- (14) Kui, S. C. F.; Chui, S. S.-Y.; Che, C.-M.; Zhu, N. *J. Am. Chem. Soc.* **2006**, *128*, 8297.
- (15) Lamansky, S.; Djurovich, P.; Murphy, D.; Abdel-Razzaq, F.; Lee, H.-E.; Adachi, C.; Burrows, P. E.; Forrest, S. R.; Thompson, M. E. *J. Am. Chem. Soc.* **2001**, *123*, 4304.
- (16) Baldo, M. A.; O'Brien, D. F.; You, Y.; Shoustikov, A.; Sibley, S.; Thompson, M. E.; Forrest, S. R. *Nature* **1998**, *395*, 151.
- (17) Baldo, M. A.; Thompson, M. E.; Forrest, S. R. *Nature* **2000**, *403*, 750.
- (18) Zhu, W.; Mo, Y.; Yuan, M.; Yang, W.; Cao, Y. *Appl. Phys. Lett.* **2002**, *80*, 2045.
- (19) Tsuzuki, T.; Tokito, S. *Adv. Mater.* **2007**, *19*, 276.

and π - π interactions were introduced with π -conjugated N- and C-donor ligands, then the emission may be governed by the whole crystal rather than by an individual molecule.^{15,20,21}

In this Article, we report the first example of a cyclometalated heteroleptic iridium complex PIr(qnx) (iridium(III) bis(2-phenylpyridinato-N,C^{2'})(quinoxaline-2-carboxylate)) that has unique and fast vapochromic and vapoluminescent behaviors. PIr(qnx) has been found to exist as both black and red (visible to the naked eye) forms in the solid state. It is interesting that the black form changed to the red form upon its exposure to acetonitrile or propionitrile vapor whereas no response was observed when it was exposed to other VOCs.

Experimental Section

Synthesis. The synthetic procedure that is used to prepare PIr(qnx) involves two steps (Supporting Information). In the first step, $\text{IrCl}_3 \cdot 3\text{H}_2\text{O}$ is reacted with an excess of 2-phenylpyridine (Alfa Aesar) to produce a $[(\text{ppy})_2\text{Ir}(\mu\text{-Cl})_2]$ dimer.²² We readily converted the dimer to PIr(qnx) by replacing the bridging chlorides with a reported quinoxaline-2-carboxylate (qnx) ligand.²³

X-ray Crystallography. Single crystals of black $\text{PIr}(\text{qnx}) \cdot 0.25\text{EtOH} \cdot 0.5\text{CHCl}_3$ and red $\text{PIr}(\text{qnx}) \cdot \text{CH}_3\text{CN}$ were grown from ethanol/chloroform and acetonitrile/chloroform solutions, respectively, by slow evaporation at room temperature. The determination of the unit cell and data collection for the two crystals was performed on a Bruker SMART 1000 area detector using graphite-monochromated Mo K α radiation ($\lambda = 0.71073 \text{ \AA}$) at 293(2) K. Structures were solved by direct methods and by successive Fourier difference syntheses (SHELXS-97) and were refined by a full-matrix least-squares procedure on F^2 with anisotropic thermal parameters for all non-hydrogen atoms (SHELXL-97).^{24,25}

Instruments and Measurements. ¹H NMR spectra were recorded on an ARX-400 NMR spectrometer. Chemical shift data for each signal were reported in ppm units with tetramethylsilane (TMS) as an internal reference, where δ (TMS) = 0. Elemental analyses were performed on a vario EL instrument. The UV-vis absorption spectra and the diffuse-reflectance spectra were measured on a Shimadzu UV-3100 spectrometer. The PL spectra and the phosphorescence decay lifetime were recorded on an Edinburgh Analytical Instruments lifetime and steady-state spectrometer (FLS920). Detailed vapochromic and vapoluminescence experiments were completed as follows. The black form was obtained by purifying the crude product, which was photographed in both ambient light and UV light (365 nm) (Figure 4b,d). The emission spectra and diffuse-reflectance spectra were also measured. The black form was exposed to acetonitrile vapor at room temperature (293 K) for 20, 40, 60, and 600 s, and the time evolution of the luminescence spectra was obtained (Figure 5). In addition, photographs in ambient light and UV light (365 nm) (Figure 5a,c) and the diffuse-reflectance spectra (Figure 5) of the fully transformed red form were recorded.

(20) Braga, D.; Grepioni, F.; Desiraju, G. R. *Chem. Rev.* **1998**, *98*, 1375.

(21) Zhang, H. Y.; Zhang, Z. L.; Ye, K. Q.; Zhang, J. Y.; Wang, Y. *Adv. Mater.* **2006**, *18*, 2369.

(22) Nonoyama, M. *Bull. Chem. Soc. Jpn.* **1974**, *47*, 767.

(23) Harms, A. E. *Org. Process Res. Dev.* **2004**, *8*, 666.

(24) Sheldrick, G. M. *SHELXS-97 Program for Solution of Crystal Structures*; University of Göttingen: Göttingen, Germany, 1997.

(25) Sheldrick, G. M. *SHELXL-97, Program for Refinement of Crystal Structures*; University of Göttingen: Göttingen, Germany, 1997.

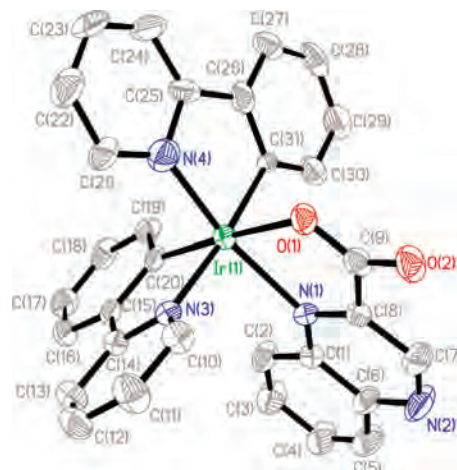


Figure 1. Crystal structure of the black $\text{PIr}(\text{qnx}) \cdot 0.25\text{EtOH} \cdot 0.5\text{CHCl}_3$. The measurement temperature was 294 K, and the thermal ellipsoids for the image represent 30% probability. The hydrogen atoms and solvents are omitted for clarity.



Figure 2. Crystal structure of the red $\text{PIr}(\text{qnx}) \cdot \text{CH}_3\text{CN}$. The measurement temperature was 293 K, and the thermal ellipsoids for the image represent 30% probability. The hydrogen atoms and solvents are omitted for clarity.

Computational Details. Theoretical calculations for the qnx dimers were carried out on with the Gaussian 03 program package.²⁶ The coordinates of the ligands came from the crystal structures, in which the crystal environment is imprinted in the conformations of ligands. We performed single point energy calculations by using the B3LYP hybrid functional and 6-311++G** basis set. To

(26) Frisch, M. J.; Trucks, G. W.; Schlegel, H. B.; Scuseria, G. E.; Robb, M. A.; Cheeseman, J. R.; Montgomery, J. A., Jr.; Vreven, T.; Kudin, K. N.; Burant, J. C.; Millam, J. M.; Iyengar, S. S.; Tomasi, J.; Barone, V.; Mennucci, B.; Cossi, M.; Scalmani, G.; Rega, N.; Petersson, G. A.; Nakatsuji, H.; Hada, M.; Ehara, M.; Toyota, K.; Fukuda, R.; Hasegawa, J.; Ishida, M.; Nakajima, T.; Honda, Y.; Kitao, O.; Nakai, H.; Klene, M.; Li, X.; Knox, J. E.; Hratchian, H. P.; Cross, J. B.; Bakken, V.; Adamo, C.; Jaramillo, J.; Gomperts, R.; Stratmann, R. E.; Yazyev, O.; Austin, A. J.; Cammi, R.; Pomelli, C.; Ochterski, J. W.; Ayala, P. Y.; Morokuma, K.; Voth, G. A.; Salvador, P.; Dannenberg, J. J.; Zakrzewski, V. G.; Dapprich, S.; Daniels, A. D.; Strain, M. C.; Farkas, O.; Malick, D. K.; Rabuck, A. D.; Raghavachari, K.; Foresman, J. B.; Ortiz, J. V.; Cui, Q.; Baboul, A. G.; Clifford, S.; Cioslowski, J.; Stefanov, B. B.; Liu, G.; Liashenko, A.; Piskorz, P.; Komaromi, I.; Martin, R. L.; Fox, D. J.; Keith, T.; Al-Laham, M. A.; Peng, C. Y.; Nanayakkara, A.; Challacombe, M.; Gill, P. M. W.; Johnson, B.; Chen, W.; Wong, M. W.; Gonzalez, C.; Pople, J. A. *Gaussian 03*, revision C.02; Gaussian, Inc.: Wallingford, CT, 2004.

Table 1. Crystallographic Data for the Black $\text{PIr}(\text{qnx}) \cdot 0.25\text{EtOH} \cdot 0.5\text{CHCl}_3$ and the Red $\text{PIr}(\text{qnx}) \cdot \text{CH}_3\text{CN}$

	$\text{PIr}(\text{qnx}) \cdot 0.25\text{EtOH} \cdot 0.5\text{CHCl}_3$	$\text{PIr}(\text{qnx}) \cdot \text{CH}_3\text{CN}$
empirical formula	$\text{C}_{32}\text{H}_{23}\text{Cl}_{1.5}\text{IrN}_4\text{O}_{2.25}$	$\text{C}_{33}\text{H}_{24}\text{IrN}_5\text{O}_2$
fw	744.92	714.77
cryst syst	monoclinic	monoclinic
space group	$P2(1)/n$	Pc
a (Å)	9.573(2)	18.893(4)
b (Å)	18.982(5)	9.7035(19)
c (Å)	18.032(5)	15.489(3)
α (deg)	90.00	90.00
β (deg)	105.146(5)	102.79(3)
γ (deg)	90.00	90.00
V (Å ³)	3163.0(14)	2769.1(10)
Z	4	4
D_{calcd} (g/cm ³)	1.564	1.714
$F(000)$	1454	1400
θ range (deg)	2.15–25.02	1.11–27.87
index ranges	$-11 \leq h \leq 9$ $-22 \leq k \leq 22$ $-21 \leq l \leq 20$	$-24 \leq h \leq 19$ $-12 \leq k \leq 12$ $-20 \leq l \leq 19$
GOF on F^2	1.039	1.070
R ($I > 2\sigma(I)$)	0.0404	0.0427
R (all data)	0.0723	0.0524

characterize the molecular interactions, we derived the molecular electrostatic potential (MEP) surfaces from the calculated electron density. To understand the different intensities in the black form and the red form, we calculated the electronic coupling matrix element (V) between the HOMOs of the π - π dimers to estimate the coupling between two monomers.²⁷ We explicitly calculated this element by using the energy splitting in dimer (ESD) method with the simplification by applying Koopmans' theorem.^{28–32}

Results and Discussion

X-ray Crystallographic Study. The crystal structures of both the black and the red forms have been determined by X-ray diffraction,³³ and the crystal structures of the black $\text{PIr}(\text{qnx}) \cdot 0.25\text{EtOH} \cdot 0.5\text{CHCl}_3$ and the red $\text{PIr}(\text{qnx}) \cdot \text{CH}_3\text{CN}$ are shown in Figures 1 and 2, respectively. The $\text{PIr}(\text{qnx})$ molecule consists of two phenylpyridine fragments as cyclometalated ligands and one quinoxalinate as an ancillary ligand ranging in a distorted octahedral geometry around the iridium atom. Crystallographic data for the black and the red forms are given in Table 1, and Table 2 lists important bond lengths and angles for both forms.

The solid-state packing framework of the black $\text{PIr}(\text{qnx}) \cdot 0.25\text{EtOH} \cdot 0.5\text{CHCl}_3$ viewed from the b axis is shown in Figure 3. For the black crystal, the two qnx ligands are composed of OFF (offset face-to-face) motifs, and these OFF dimers form layers along the bc plane. Additionally,

Table 2. Selected Bond Lengths (Å) and Angles (deg) for the Black Form and the Red Form

	$\text{PIr}(\text{qnx}) \cdot 0.25\text{EtOH} \cdot 0.5\text{CHCl}_3$	$\text{PIr}(\text{qnx}) \cdot \text{CH}_3\text{CN}$
Ir(1)–C(31)	2.026(7)	2.030(10)
Ir(1)–C(20)	1.996(8)	1.999(12)
Ir(1)–N(3)	2.049(6)	2.045(9)
Ir(1)–N(4)	2.026(8)	2.004(11)
Ir(1)–N(1)	2.227(6)	2.191(10)
Ir(1)–O(1)	2.162(5)	2.152(7)
N(4)–Ir(1)–C(31)	81.2(3)	80.7(4)
N(3)–Ir(1)–C(20)	80.0(3)	80.4(4)
N(1)–Ir(1)–O(1)	75.8(2)	76.8(3)
N(1)–Ir(1)–N(4)	168.1(3)	167.4(4)
C(31)–Ir(1)–N(3)	173.8(2)	173.5(4)
O(1)–Ir(1)–C(20)	174.5(3)	174.4(4)

the layers stack along the a direction and form channels of 6.5×4.0 Å² along the b direction. These channels are large enough to allow ethanol and chloroform to reside simultaneously.

The solid-state packing framework of the red $\text{PIr}(\text{qnx}) \cdot \text{CH}_3\text{CN}$ crystal viewed from the c axis and the layer viewed from the a axis are shown in Figure 4. For the red crystal, the packing is considered to be a hexagonal close-packing arrangement of the molecules in which the hexagonal layer is along the bc plane. These layers pack along the a direction in ABAB style, and the adjacent layers are related to each other by the 2-fold screw axis and form an OFF stack.

Vapochromic and Vapoluminescent Behaviors. The black form was found to exhibit weak luminescence under UV light, with a broadband centered at 692 nm and a decay lifetime of 43 ns. The black form can immediately translate into the red form after it exposed to acetonitrile liquor, or it can translate into the red form over a period of only 1 min after it is exposed to acetonitrile vapor at room temperature. After its exposure to acetonitrile vapor, the black crystal not only changes color but also loses its crystallinity and becomes a red alveolate form. The red form exhibits an intense luminescence when it is exposed to UV light, with an emission peak centered at 654 nm and a decay lifetime of 130 ns. The emission intensity of the red form is much stronger than that of the black form. This difference in the emission intensity indicates that the title complex has an evident sensitivity in detecting the acetonitrile vapor. Photographic and luminescence images and solid PL spectra of both the black and the red forms of $\text{PIr}(\text{qnx})$ are shown in Figure 5.

The changes in the vapochromic and vapoluminescence processes were verified by diffuse reflectance, IR, and ¹H NMR. After absorbing acetonitrile, the black form became red; the change in color can be evidenced by different diffuse-reflectance spectra of both forms (Supporting Information, Figure S1). The black form exhibits a broadband in the IR spectrum at ~ 3400 cm⁻¹ that is attributed to the O–H vibration of ethanol, whereas the red form exhibits a band at 2248 cm⁻¹ that corresponds to acetonitrile and does not exhibit a band around 3400 cm⁻¹ (Supporting Information, Figure S2). This difference in the IR indicates that the ethanol in the black crystal was substituted by acetonitrile. A chemical shift (δ , 1.99) in the ¹H NMR spectroscopy also indicated that acetonitrile was absorbed.

(27) *Electron Transfer: From Isolated Molecules to Biomolecules*; Jortner, J., Bixon, M., Eds.; Advances in Chemical Physics Series; Wiley: New York, 1999; Vols. 106–107.

(28) Liang, C.; Newton, M. D. *J. Phys. Chem.* **1992**, *96*, 2855.

(29) Kwon, O.; Coropceanu, V.; Gruhn, N. E.; Durivage, J. C.; Laquindanum, J. G.; Katz, H. E.; Cornil, J.; Brédas, J. L. *J. Chem. Phys.* **2004**, *120*, 8186.

(30) Newton, M. D. *Chem. Rev.* **1991**, *91*, 767.

(31) Brédas, J.-L.; Beljonne, D.; Coropceanu, V.; Cornil, J. *Chem. Rev.* **2004**, *104*, 4971.

(32) Coropceanu, V.; Cornil, J.; da Silva Filho, D. A.; Olivier, Y.; Silbey, R.; Brédas, J.-L. *Chem. Rev.* **2007**, *107*, 926.

(33) CCDC 640981 and 640982 contain the supplementary crystallographic data for this Article. These data can be obtained free of charge via www.ccdc.cam.ac.uk/data_request/cif, by e-mailing data_request@ccdc.cam.ac.uk, or by contacting the Cambridge Crystallographic Data Centre, 12 Union Road, Cambridge, CB2 1EZ, U.K.; fax: +44 1223 336033.

To examine the selectivity of this vapochromic and vapoluminescent behavior, the black form was exposed to a series of vapors at room temperature, including ethyl ether, acetic acid, ethyl acetate, methanol, ethanol, 2-propanol, acetone, pyridine, tetrahydrofuran, dichloromethane, chloroform, petroleum ether, hexane, benzene, iodomethane, and propionitrile. We found that the black form of PIr(qnx) yielded no response for all of the above VOCs except for propionitrile, even after an exposure for several hours; thus, the observed vapochromic and vapoluminescent behaviors of PIr(qnx) are fairly unique compared with those of other reported complexes.^{3,4,10,11} Although it is difficult for the red crystal to revert to the black form, even after drying in a vacuum oven for a long period of time (days), it is convenient to translate the red form to the black form by dissolving PIr(qnx) in chloroform and then vaporizing the solvent.

To understand the selectivity of PIr(qnx) for acetonitrile, we investigated the effect of solvent molecules in both crystals in detail (Supporting Information, Figure S3). Although the ethanol molecule is surrounded by PIr(qnx) molecules in the black crystal, the shortest distance between the oxygen of ethanol and the hydrogen atoms of PIr(qnx) is 3.27 Å, and thus the potential interaction between the solvent and the complex is very weak. For the red crystal, every acetonitrile molecule is involved in several interactions with its neighbors. These interactions may contain the N \cdots H–C-type and possible π (C \equiv N) \cdots H–C-type weak hydrogen bonds, and the corresponding distances vary from 2.98 to 3.14 Å. Although the individual hydrogen bonding is weak, the total interaction energy may still be large because of the cooperativity effect among these weak hydrogen bonds. This may account for the fact that once the acetonitrile vapor arrived at the black form the ethanol was replaced and the packing manner was changed.

Offset Face-to-Face Motifs Comparing Two Forms. It should be noted that both the black PIr(qnx)·0.25EtOH·0.5CHCl₃ and the red PIr(qnx)·CH₃CN have the same photophysical properties when they are dissolved in dichloromethane, and the emission is very weak because the ancillary ligand qnx is introduced. The DFT calculation of a single molecule shows that the HOMO consists of a mixture of Ir–d and phenyl– π ppy orbitals whereas the LUMO is mainly distributed on qnx orbitals (Supporting Information, Figure S4). This may be the reason that a strong MLCT transition similar to that of other iridium complexes such as iridium(III) bis(2-phenylpyridinato-N,C^{2'})(acetylacetonate) [Ir(ppy)₂(acac)], whose LUMO is mainly distributed on pyridine– π ppy orbitals, is not observed. However, in the solid state, both the red form and the black form have stronger emissions than the diluted solution state, and thus the transition of the solid state may originate from the aggregation-induced phosphorescence emission.³⁴ Furthermore, the emission intensity of the red form is much stronger than that of the black form, and an important difference between the crystal structures of the black and red forms of

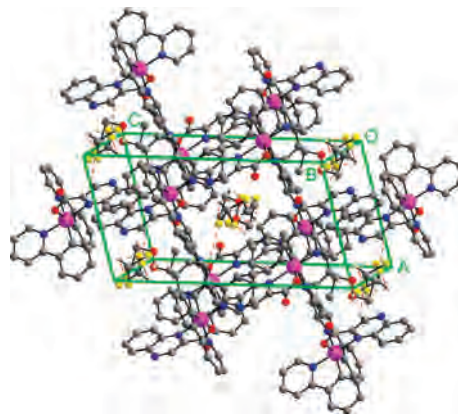


Figure 3. Solid-state packing of the black PIr(qnx)·0.25EtOH·0.5CHCl₃ crystal. Some of the hydrogen atoms are omitted for clarity. Iridium, nitrogen, oxygen, carbon, hydrogen, and chlorine are purple, blue, red, gray, white, and yellow, respectively.

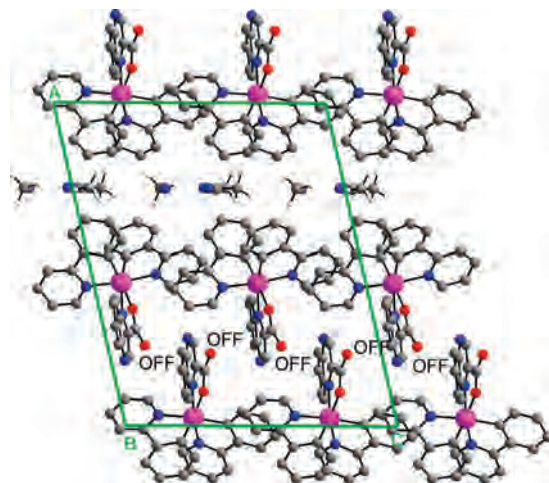


Figure 4. Solid-state packing of the red PIr(qnx)·CH₃CN crystal. Some of the hydrogen atoms are omitted for clarity. Iridium, nitrogen, oxygen, carbon, and hydrogen are purple, blue, red, gray, and white, respectively.

PIr(qnx) is the type of π – π stacking in the OFF motifs, which may be the key in understanding the sharp differences in the PL properties. Herein, DFT was employed in investigating the characteristics of the π – π interactions. For simplicity and computational cost, only the qnx dimers are considered to be models. For the black form, the coordinated qnx ligand has a relatively well-defined plane with a maximum angle of ca. 2.8°, and the π – π stacking exists as an antiparallel pattern. For the red form, the qnx ligand is a contorted plane with a maximum angle of ca. 13.7°, and the π – π stacking shows a parallel pattern (Supporting Information, Figure S5). The above observation indicates that the π – π stacking in the black form favors a dipole–dipole interaction between the qnx ligands and has a shorter distance (ca. 3.4–3.5 Å). The red form has an unfavorable dipole–dipole arrangement so that its π – π distance (ca. 3.5–3.7 Å) is longer than that of the black form. This coincides with the calculation results that were obtained from the DFT for the electrostatic potential (Figure 6).

Usually, a large electronic coupling between the HOMOs of the π – π dimer may indicate an efficient energy transfer, which leads to a stronger emission intensity in a dimer

(34) Zhao, Q.; Li, L.; Li, F.; Yu, M.; Liu, Z.; Huang, C. *Chem. Commun.* 2008, 685.

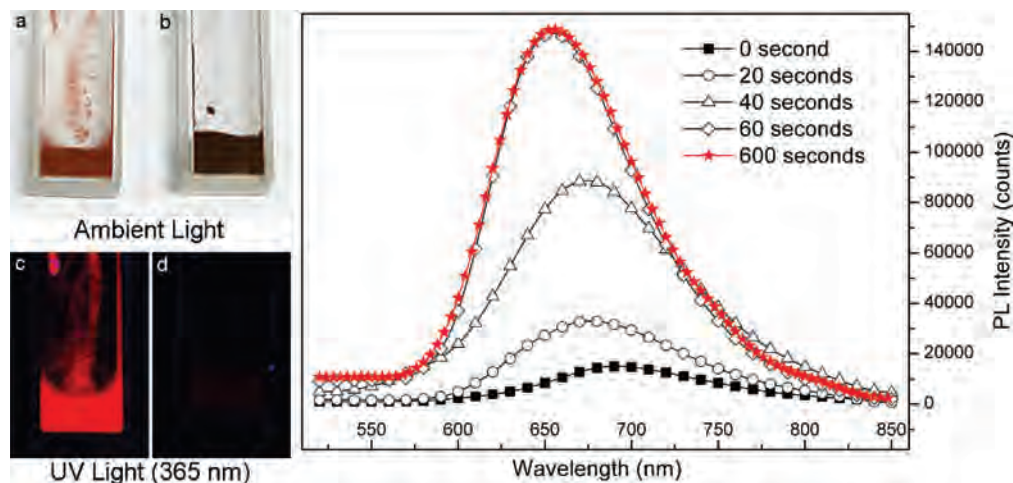


Figure 5. Photographic images of (a) the red form and (b) the black form of PIr(qnx). Luminescence images of (c) the red form and (d) the black form of PIr(qnx). Photoluminescence spectra of the black form exposed to acetonitrile vapor at different periods of time.

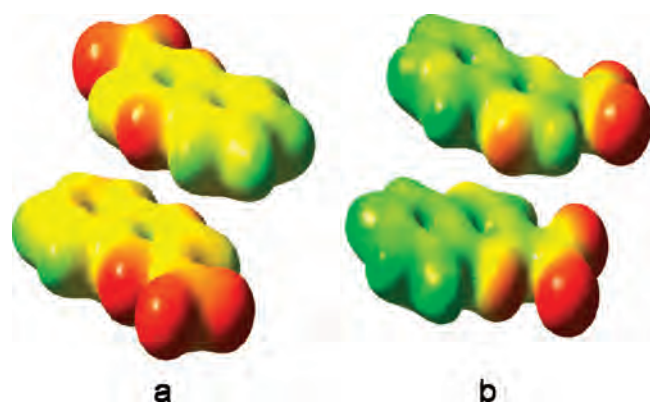


Figure 6. Calculated electrostatic potential on the isodensity surface of the π - π qnx dimers in (a) the black form and (b) the red form. The isodensity contours were plotted for 0.02 electron/ b^3 .

system.²⁷ Herein, we evaluated the electronic coupling in both the black form and the red form. For the black form, the electronic coupling matrix element of the π - π dimer is found to be trivial (0.0016 eV). On the contrary, the same quantity in the red form is much larger (0.0632 and 0.1506 eV for different OFF dimers), which suggests an enlarged overlap between the HOMOs of the π - π dimer. This also suggests that the efficiency of the energy transfer between the two qnx ligands in the red form is much higher than that in the black form. This coincides with the phenomenon that the emission intensity of the red form is much higher than that of the black form.²⁷

In addition, the electronic coupling of the LUMOs of the π - π dimer was also investigated as a factor in understanding the different photophysical properties between the black form and the red form. Data show that the electronic coupling matrix element between the LUMOs of the two monomers in the black form (0.109 eV) is much larger than that in the red form (0.079 and 0.068 eV for different OFF dimers). On the basis of crystal structures and the above-mentioned result, a schematic representation of the red-shifted emission spectrum and the quenching process in the black form is diagrammed in Figure 7. Because the intermolecular force is stronger in the black form, the distance between two qnx ligands is

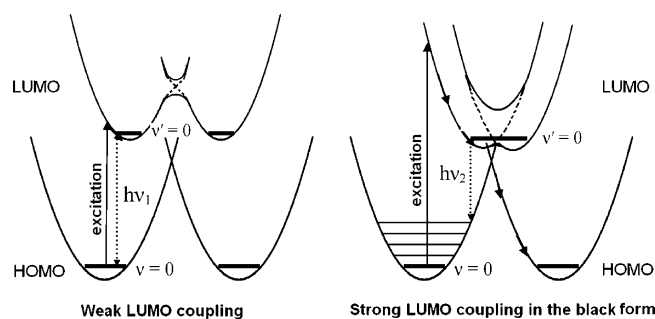


Figure 7. Schematic representations of the red-shifted emission spectrum and the quenching process due to the strong coupling between the LUMOs of the two monomers in the black form.

much shorter, the coupling strength between the LUMOs of the two monomers that locate mainly on the qnx is much stronger, and the potential curve of the excited state is greatly changed (Figure 7, right side). As can be seen from the Figure, the transition energy gap in the black form is decreased, which coincides with the phenomenon that the black form has a longer emission wavelength. In addition, because the potential curves of the excited state in the black form are lower and are shifted because of the strong coupling, they will have a larger overlap with the vibrational levels of the ground state, which shows that the excited electron of one PIr(qnx) molecule could easily transfer to the ground state of itself or the other PIr(qnx) molecule. Because of this quenching process, we conclude that the black form has a weaker emission intensity.

Conclusions

A cyclometalated heteroleptic iridium complex PIr(qnx) has been synthesized and characterized. Density functional theory studies show that the lowest excited state of the PIr(qnx) involves the ancillary ligand qnx, which is very different from its analogous iridium complexes such as Ir(ppy)₂(acac). For this reason, the strong ³MLCT transition that is usually observed in the iridium complex cannot be observed here. It is interesting that the novel complex exhibits vapochromic and vapoluminescent behaviors in

response to acetonitrile or propionitrile vapor, and the behaviors are evident and fast. On the basis of crystallographic and DFT studies, we deduce that the black form first adsorbs acetonitrile vapor because of its porous packing structure and then the red form is formed with different color and luminescence properties and is induced by weak intermolecular interactions such as hydrogen bonding and π - π interactions.

Acknowledgment. This work was supported by the National Basic Research Program (2006CB601103) and the NNSFC (20021101, 20423005, 20471004, 50372002, and

20671006). We thank Professors Z. M. Wang, S. W. Zhang, and G. D. Zhou for the kind discussion.

Supporting Information Available: X-ray crystallographic data; synthetic procedure of Hqnx and PIr(qnx); diffuse-reflectance spectra and IR spectra of both forms; weak interactions between PIr(qnx) and solvent molecules; contour plot of HOMO and LUMO of PIr(qnx) and Ir(ppy)₂(acac); and offset face-to-face motifs in both the black and red forms. This material is available free of charge via the Internet at <http://pubs.acs.org>.

IC702141H